ACOUSTIC RESULTS OF THE BOEING MODEL 360 WHIRL TOWER TEST

Michael E. Watts
Rotorcraft Technology Branch
NASA Ames Research Center
Moffett Field, CA USA

David Jordan
Flight Experiments Branch
NASA Ames Research Center
Moffett Field, CA USA

Abstract

In January of 1987, a whirl tower test of the Boeing Helicopter Model 360 rotor system was performed at Philadelphia, Pennsylvania. The Model 360 advanced high performance 4-bladed rotor system is composed of an articulated hub, blades that employ advanced airfoils, and a 3:1 taper on the outboard 10% of the rotor span. The tandem rotor Model 360 is designed to be a 200+ knot helicopter of primarily composite material construction.

In addition to the whirl-tower performance measurements, acoustic data were acquired from seven microphones. Three of the microphone locations were carefully selected to correspond with three geometrically similar locations of microphones from the Model 360 1/5 scale wind tunnel test conducted in The Netherlands. Two of these microphones were located 3.0 rotor diameters from the rotor hub, one 6° and one 15° down from the rotor disk. The third similar position microphone was at 4.6 rotor diameters and 15° down from the rotor disk.

Comparison of the results of the whirl-tower test with theory show that the theoretical prediction accuracy varies with microphone position and the inclusion of ground reflection. The prediction error, with ground reflection included, ranged from 0 to 40% of the measured signal peak-to-peak amplitude. This peak-to-peak accuracy is on the order of that obtained by previous anechoic facility model scale comparisons of experiment and theory.

Introduction

Acoustic prediction has become important in the design of rotorcraft as civil environments and battlefield detectability become increasingly important issues. Just as stealth technology is incorporated into aircraft at the design level in the form of reduced radar cross section, electronic emissions, and infrared signatures, reduced acoustic emissions have become a major design goal in the reduction of rotorcraft detectability and community annoyance. To accomplish this task, predictive codes have become more sophisticated in recent years. However, to prove the validity and worth of these codes, accurate experimental data is essential. In many cases, rotor tests are designed with the primary goal of obtaining performance data with acoustics data being obtained as a target of opportunity. In these cases, the experimental setup is usually not optimized for acoustics data acquisitions to minimize background noise and reduce reflected signals. Even when the effort is made to acoustically treat the experimental test stand, the ground surface still provides a reflection plane which distorts the data. To use such data for detailed waveform shape and amplitude research, the contribution of reflected signals must be addressed in theoretical predictions.

The Boeing Helicopter Model 360 front rotor was tested on the Boeing Helicopter Engineering Whirl Tower (BHEWT, Fig 1) located next to the Philadelphia International Airport. The primary purpose of the test was obtaining hover performance data and an acceptance endurance test. Acoustics data were acquired during the whirl tower test as a target of opportunity.

Rotor Description

The 4-bladed rotors for the Model 360 (Ref 1) are 49.7 ft (15.15 m) in diameter. The rotor blades incorporate airfoils from the VR-12 and -15 family of airfoil sections, the newest representatives of Boeing Helicopter's in-house airfoil design evolution. The VR-12 (10.6% thick) section is used from the root cut-out to 85% radius, at which point the transition begins to the VR-15 (8% thick) section at the blade tips. A constant chord is used from 28% radius to 90% radius at which point a 3:1 taper begins and is continued to the blade tips. The twist distribution is +6.5 degrees at 23% radius, -1.28 degrees at 86% radius, and -3.7 degrees at the blade tips, with linear transitions between these stations. The concept of the advanced rotor design was to utilize optimized values of blade taper and twist to improve hover performance while using the advanced VR-12 and -15 airfoil sections to improve cruise performance.

Experimental Setup

The rotor hub is mounted at a height of 50 ft (15.24 m) above ground level on the BHEWT which has a conical structure. Electric motors power a spiral bevel gear and a four speed gear box. The gear box powers a drive shaft which in turn powers the rotor hub. For the whirl-test, rotor thrust, torque and speed were measured as well as trim actuator loads. Rotor blade instrumentation consisted of 6 flap, 4 chord and 3 torsion strain gage bridges. In addition, blade pitch, flap and lead/lag angles, and pitch link loads were measured.

Rotor hover performance data was acquired during rotor speed sweeps at constant collective actuator settings of approximately 0, 8, 10, 11, 12, 13, 14, and 15 degrees, and a collective actuator sweep at a constant nominal rotor speed of 256 rpm. The thrust and torque data obtained indicated a maximum Figure of Merit of 0.758. Detailed results of the performance measurements are presented in reference 2.

A seven-microphone array was used for the acoustic portion of the test. The positions for these microphones (#1,2, and 3) were geometrically similar to positions used during the Duits-Nederlandse Windtunnel (DNW) test of a model scale 360 rotor (Ref 3) and two microphones (#4 and 6) matched positions used during tests of other rotors on the BHEWT. The remaining microphones (#5 and 7) were set in an inverted position over aluminum ground planes. These microphone positions are shown in figure 2 and the relation of the microphones to the DNW positions is shown in table I. The microphones used were pre-amplifier powered, 1/2 inch condenser type, each covered with a foam windscreen. A 14-track, 1 inch (2.54 cm) tape recorder was used at a tape speed of 30 in/sec (0.762 m/sec) to record the microphone signals. The amplifiers in the recorder were set for Inter-Range Instrumentation Group (IRIG) intermediate band FM recording. A frequency response calibration of the tape recorder produced a curve that was flat to within ± 1 dB from 0-10 kHz. Single frequency calibrations at 1,000 Hz, 114 dB were performed at the beginning and end of the test. Along with acoustic data, a rotor 1/rev signal, voice inputs, and a time-code signal were recorded.

Ambient conditions during the acquisition of acoustic data consisted of low winds and an average temperature of 33 F (0.6 C) with snow covering the ground to a depth of approximately 1 ft (0.3 m).

Theoretical Modeling

The theoretical code used for the prediction of generated acoustics for this paper is called Rotor Noise (RTN) and was developed by Aggarwal and Schmitz (Ref 4). The theory used in RTN is derived from first principles based on the Ffowcs Williams and Hawkings equations as found in reference 5. (See reference 6 for details of this derivation and implementation into RTN.) The RTN code as developed in reference 6 had no capacity for the inclusion of the effects of reflected waves on the resultant wave as seen by the observer or microphone. The correlation of RTN with the DNW Model 360 hover data performed in reference 4 showed good correlation of theory and experiment for low- to medium- hover tip Mach numbers.

Acoustics prediction depends on the quality of the input lift and drag distributions. The Analytical Methods Incorporated (AMI) free-wake lifting surface code (Ref 7) was used for generating the input distributions since no experimental values were available. The lift coefficients were obtained by adjusting the input collective angle to match the measured thrust. The integrated drag distribution was corrected to match the measured torque and this correction was applied to the drag distribution in RTN.

Acoustic data acquired in non-anechoic facilities such as the BHEWT will have reflections which modify the measured acoustic wave. Even near-anechoic facilities such as the DNW will have reflections in certain microphone locations, as noted in reference 4. Because of these considerations, the RTN code was modified to include reflected paths. Normally, attenuation of the reflected signal must be included to properly model the absorption characteristics of the reflecting surface. As noted previously, the test was performed with one foot of snow cover over frozen ground. Albert and Orcutt have shown, in reference 8, that this ground cover condition will result in no signal attenuation below 35 Hz at the microphone distances used during the whirl test. Since the primary contributors to the hovering acoustic wave shape and amplitude are the 4- and 8- per rev frequencies, nominally 17.6 and 35.2 Hz, no attenuation of the reflected signal was included in the results used for this paper.

Experimental Data

The acoustics data acquired was analyzed using the Macintosh-based Acoustic Laboratory Data Acquisition/Analysis System (ALDAS, Ref 9). This system has one 12- and two 16- bit analog-to-digital cards, which are controlled by the ALDAS program written at NASA Ames Research Center. The data were sampled at 2048 samples per revolution which resulted in sample rates of approximately 9000 samples per second. All data were analog filtered at 2500 Hz before sampling to prevent aliasing.

Figure 3 (a and b) shows the variation in the wave shape of the raw data for one test condition (M_{tip}=0.631 and C_T/σ=0.0797). The variation of the signal is due to the unsteadiness of the flow field and the high background noise of the BHEWT. Since the hover condition is primarily a low frequency phenomenon, the acoustic data was filtered at a relatively low frequency. The cutoff frequency of this digital low-pass filter was determined by first averaging a data trace for 64 cycles, and then performing a spectral analysis of the resultant cycle. As can be seen from figure 4, the point where the curve-fit to the first 24 harmonics intersects the medium line for the signal out to 1000 Hz is at 115 Hz. All data was digitally low-pass filtered at this frequency before cycle averaging was performed. Data was then cycle averaged for at least 32 cycles and usually 64 cycles. Figure 5 shows the effect of this process on the same data as shown in figure 3.

Test points in the acoustics portion of the whirl test fell within the range of 0.354 to 0.665 hover tip Mach number and 0.0469 to 0.1223 C_T/σ. Efforts were made to match test parameters from the Army/Boeing/NASA DNW test (Ref 3). Figure 6 shows the test matrix as a function of hover tip Mach number versus C_T/σ. The solid line indicates the bounds of the data taken in the DNW hover test and the diamonds show the actual test points of the whirl tower test. Data indicated by solid diamonds are discussed in detail below.

Discussion of Results

This paper will concentrate on data for a range of thrust conditions at two hover tip Mach numbers, 0.543±0.004 and 0.630±0.001, which are indicated by the solid diamonds in figure 6. The banding of the Mach numbers presented is because of the courseness of the speed control of the BHEWT. In addition, the three microphones which closely matched locations from the DNW test will be used to provide commonality. Both wave shape and peak-to-peak amplitude comparisons of experiment with theory will be made.

Averaged experimental and predicted waveforms are presented in figures 7 thru 12. Both the direct path and direct plus reflected (dual) paths are also presented to show the effects of the reflection on the wave shape.

The reflected wave causes the calculated waveform to more closely match the positive and negative slopes of the experimental waves for microphones two and three. This effect is evident for all conditions with the most benefit being seen in the lower thrust conditions, and degrading slightly for the higher thrusts. Higher frequencies not predicted in the theory are evident in the fundamental wave shape of the experimental data. These frequencies tend to mask the wave shape for the higher thrust conditions. Figure 13 shows a typical comparison of the spectra between a high and low thrust case. The low thrust spectrum dies out at about 80 Hz and the high thrust spectrum continues to above the filter frequency (frequency contents above 115 Hz are filter roll-off effects). Figure 14 shows a typical effect of filtering the experimental data at the 8/rev frequency (35 Hz) for microphone 3, M_{tip} of 0.630 and C_T/σ of 0.1103. Even though this filtering level shows a closer match of the theoretical and experimental curves, it is not applied to the data since it masks the higher frequency effects contained in the data and can be considered "tailoring" the results.

The phase of the reflected wave for microphone one forces a double-humped shape which is completely different from that of microphones two and three. This hump is not as obvious for the lower as for the higher Mach number cases. The correlation with theory ranges from good, as seen in figure 10, to evident but obscure as seen in figure 12. It appears that the data for this microphone have high frequency data overlaying the signal as discussed above. However, filtering the data at 35 Hz does not improve the correlation significantly.

The other consideration in comparing theory and experiment is the peak-to-peak amplitude of the signals. Figure 15 presents the peak pressure differences for the experimental and the dual-path theoretical data for microphones 1 thru 3. In examining this figure, similar results are to be noted as with the wave shape comparisons. In other words, microphones two and three had very good correlation at the low Mach number and good agreement at the higher Mach number. Microphone 1 had fair agreement for both Mach number conditions.

Figure 16 is presented to illustrate the improvement in the peak-to-peak amplitudes with the addition of the reflected wave. This figure shows the percent error of the direct-path and dual-path predictions with the measured value.

$$Percent\ Error = \frac{(Experiment - Theory)}{Experiment} x100$$

In this figure, a positive percent error represents an under prediction of amplitude. Notice that the change from the open (direct path) symbols to the closed (dual path) symbols is towards zero percent error for microphones two and three. Even though the change in curves may go through zero to the over-prediction side, this trend indicates that the addition of the reflection has a beneficial effect on the prediction of peak-to-peak amplitudes for these locations. Microphone one has the opposite trend indicating that the reflection is driving the amplitude away from the correct value. This inconsistency of microphone 1 trends with those of microphones two and three was also seen in the wave shape comparisons.

As mentioned previously, the microphone 3 position closely matches the 3.0 diameter, 15° down microphone from the DNW test. Two papers have previously compared acoustic theory to DNW 1/5 scale model data for this microphone location (Ref 4 and Ref 10). Both papers used the AMI code to generate the loads distribution for input into the theoretical codes. Reference 4 used the RTN code and reference 10 used the Rotor Acoustics Predictive Program (RAPP). Neither application included reflection effects. The DNW test Mach number used was 0.636 which is slightly different than the full scale 0.63 from the whirl test. To eliminate the effects of this difference, the results are presented in figure 17 as percent error of the peak-to-peak values. The measured value in this figure is the experimental value from the test being predicted. This figure shows that the addition of the reflected wave in the whirl tower data brings the accuracy of the peak-to-peak prediction into the same error range as that for RTN and RAPP compared with data from the anechoic DNW.

Concluding Remarks

The results presented show that the addition of a ground reflection into the predicted acoustics curves can have a significant effect on the results. For a normal hover tip Mach number, the addition of a ground reflection yields accuracies for the non-anechoic whirl-tower test data on the order of those seen for the anechoic DNW test. The common level of error could be the result of incorrectly predicted loads or limitations in the theoretical acoustics model. Application of the reflection correction must be used carefully as its effects are dependent on the phase of the reflection and the damping of the reflecting surface (Ref 8).

References

1. Hartman, L. J., Mecklin, R., and Wiesner, R., "Boeing Model 360 Advanced Technology Helicopter Design Features and Flight Test Update", Presented at the 44th Annual National Forum of the American Helicopter Society, June 1988.

2. "Whirl Tower Test of an Advanced High Performance (Model 360) Rotor", Boeing Helicopter Final Report, NASA Contract NAS 2-11966, Ames Research Center, Moffett Field, CA, 1988.

3. Dadone, L., Dawson, S., and Ekquist, D. "Model 360 Rotor Test at DNW —Review of Performance and Blade Airload Data", Presented at the 43rd Annual Forum of the American Helicopter Society, 1987.

4. Aggarwal, H.R., Schmitz, F.H., and Boxwell, D.A., "Prediction and Measurement of Low-Frequency Harmonic Noise of a Hovering Model Helicopter Rotor", Presented at the 45th Annual National Forum of the American Helicopter Society, May 1989.

5. Ffowcs Williams, J.E., and Hawkings, D.L., "Sound Generation by Turbulence and Surfaces in Arbitrary Motion", Philosophical Transactions of the Royal Society of London, Series A: Mathematical and Physical Sciences, Vol. 264, 1969, pp. 321-342.

6. Aggarwal, H.R., "Low-Frequency Helicopter Acoustic Prediction", Final Report, Aeroflightdynamics Directorate Contract NAS 2-12239, Ames Research Center, Moffett Field, CA, 1988.

7. Summa, J.M., and Maskew, B., "A Surface Singularity Method for Rotors in Hover or Climb", USAAVRADCOM TR 81-D-23, December 1981.

8. Albert, D.G., and Orcutt, J.A., "Acoustic Pulse Propagation Above Grassland and Snow: Comparison of Theoretical and Experimental Waveforms", Journal of the Acoustical Society of America, Vol. 87, No. 1, January 1990, pp. 93-100.

9. Watts, M.E., "ALDAS Users Manual", NASA TM 102831, 1990.

10. Gallman, J.H., "The Validation and Application of a Rotor Acoustic Prediction Computer Program", Proceedings of the 1990 Army Science Conference, June 1990.

Table I. Common whirl tower and DNW microphone locations.

BHEWT BV 360			DNW BV 360		
Mic	Radial Location (Dia.)	Downward Angle (°)	Mic	Radial Location (Dia.)	Downward Angle (°)
1	2.99	5.85	15	3.0	6
2	4.62	6.05	22	4.6	6
3	2.99	15.1	16	3.0	15

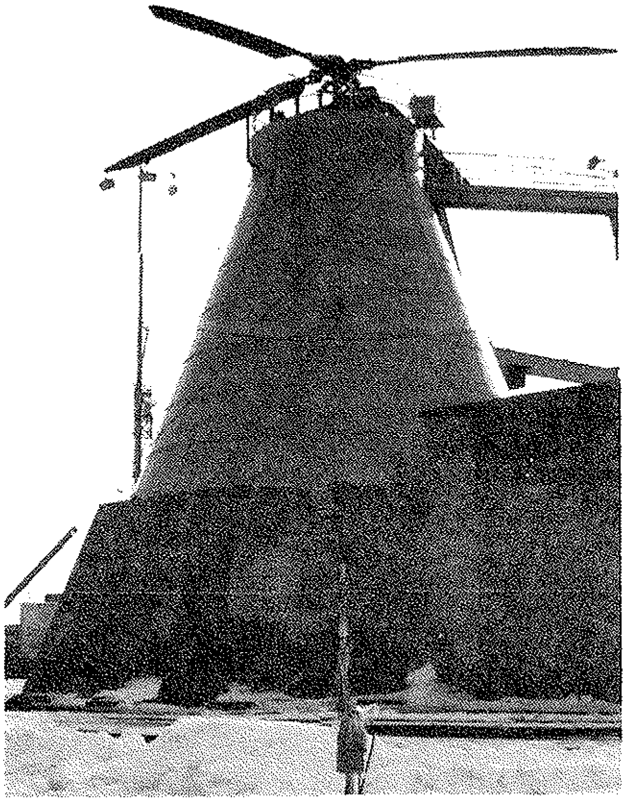

Fig 1. Boeing Helicopter Engineering Whirl Tower

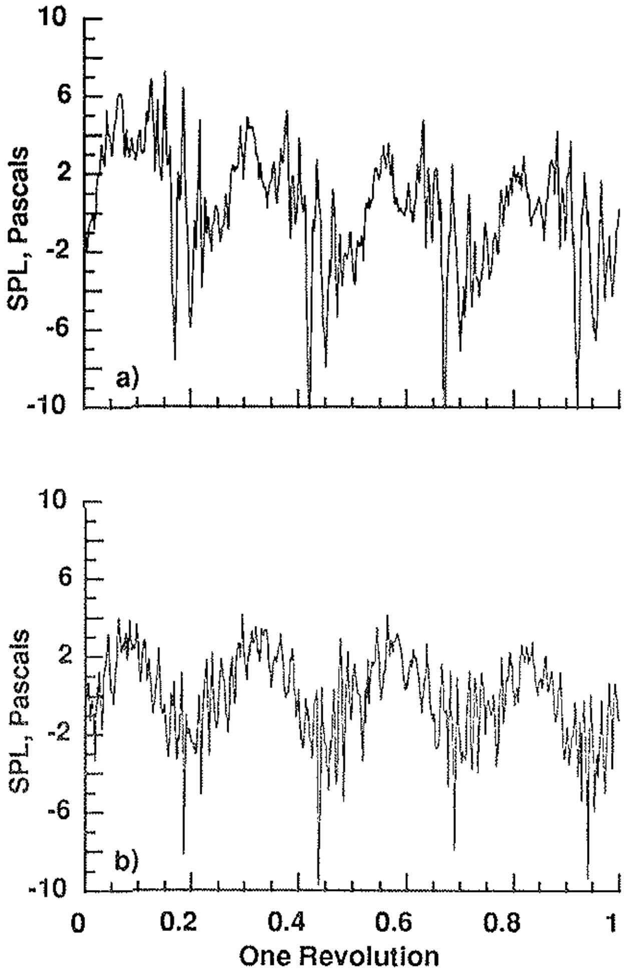

Fig 3. Examples of variation of raw data with time.

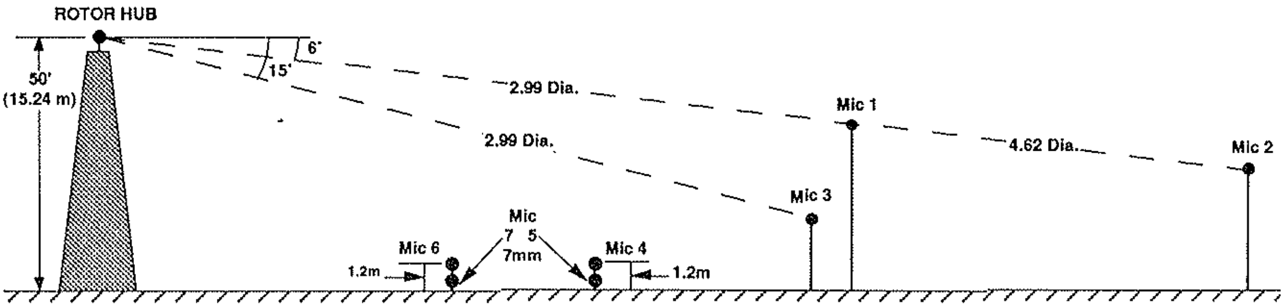

Fig 2. Sketch of microphone locations

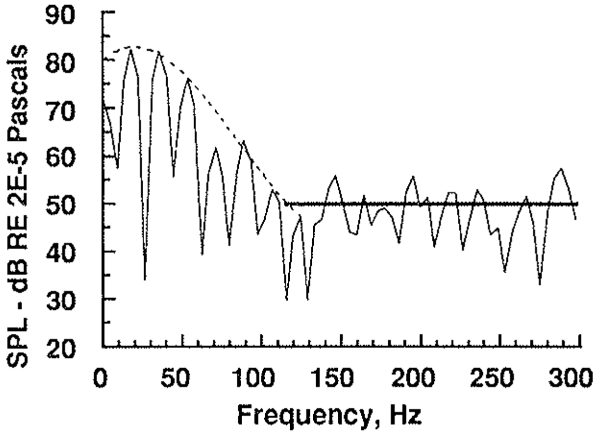

Fig 4. Spectrum used to determine filter frequency cutoff value.

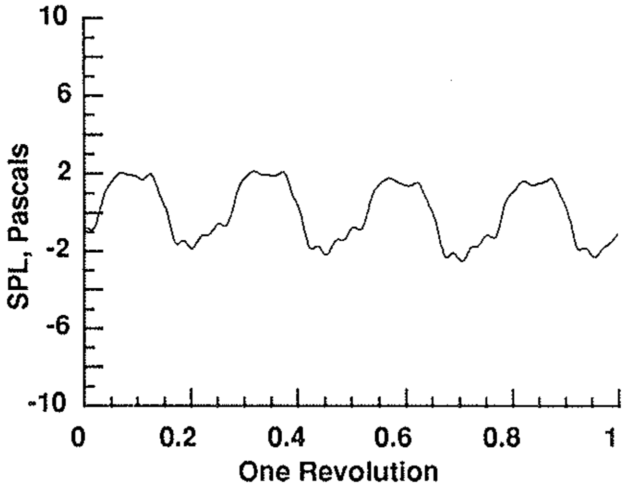

Fig 5. Data after filtering and averaging

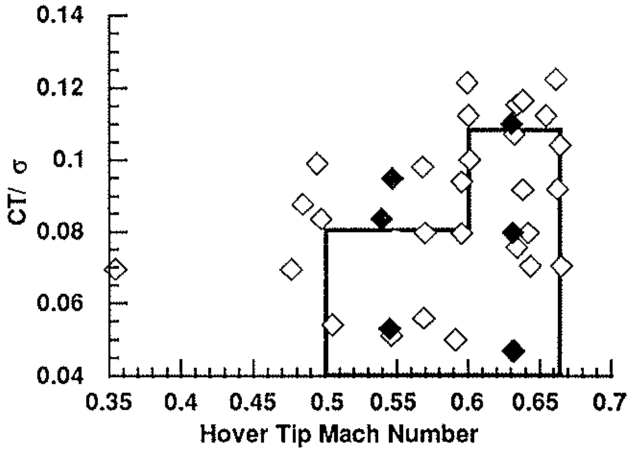

Fig 6. Data points taken for acoustics test.

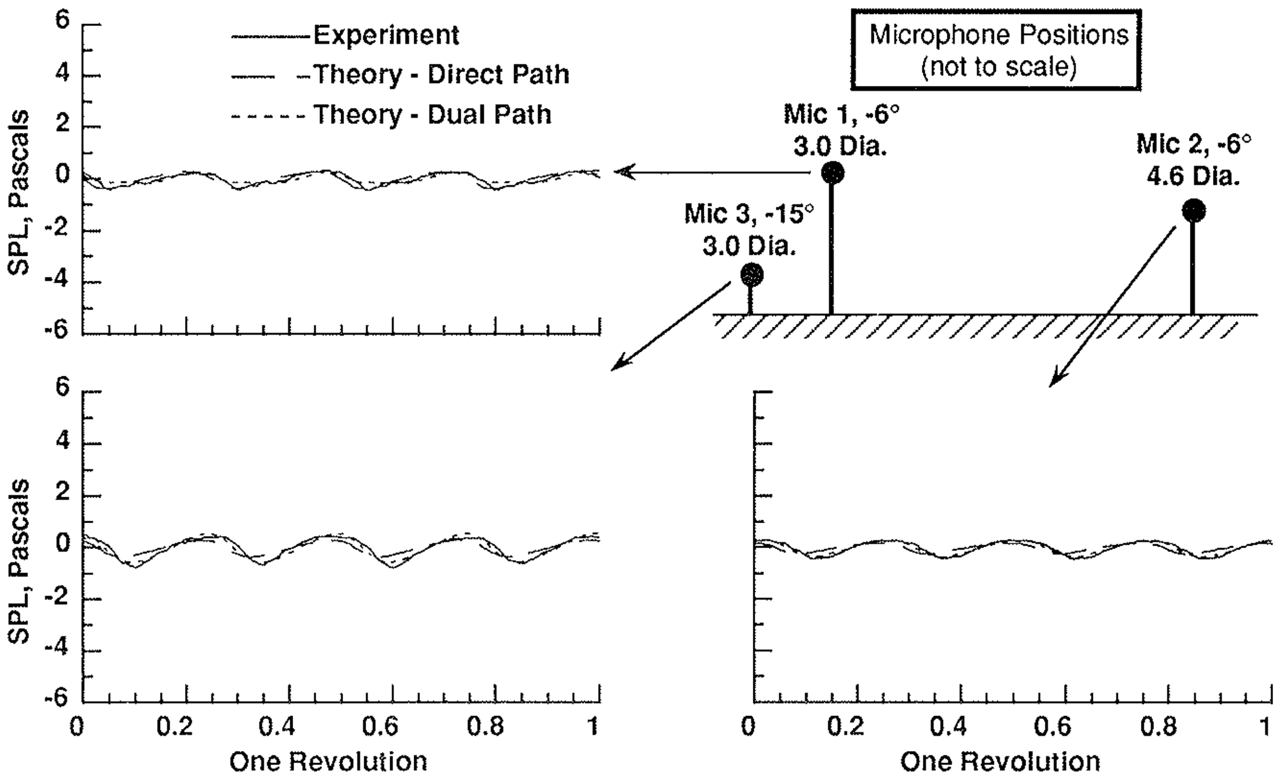

Fig 7. Experiment and theoretical wave shapes, $M_{tip} = 0.544$, $C_T/\sigma = 0.0531$.

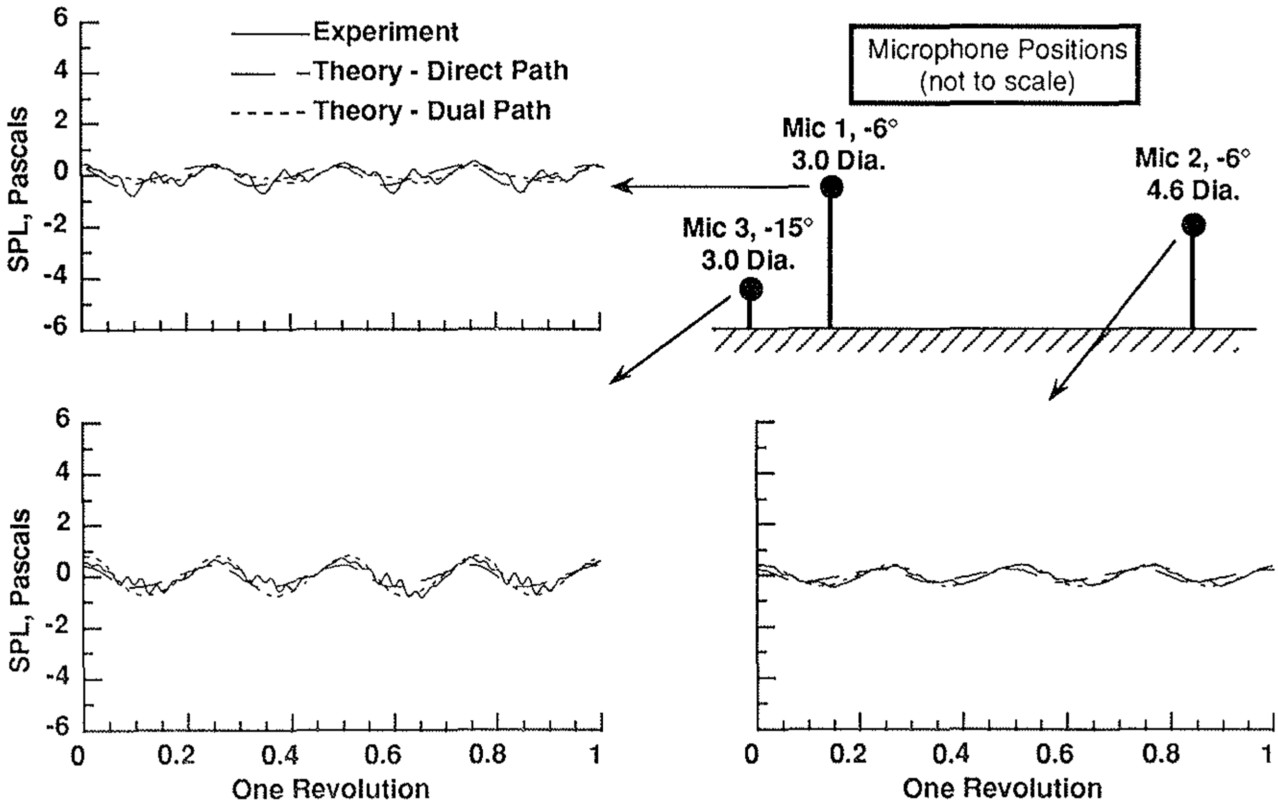

Fig 8. Experiment and theoretical wave shapes, $M_{tip} = 0.544$, $C_T/\sigma = 0.0837$.

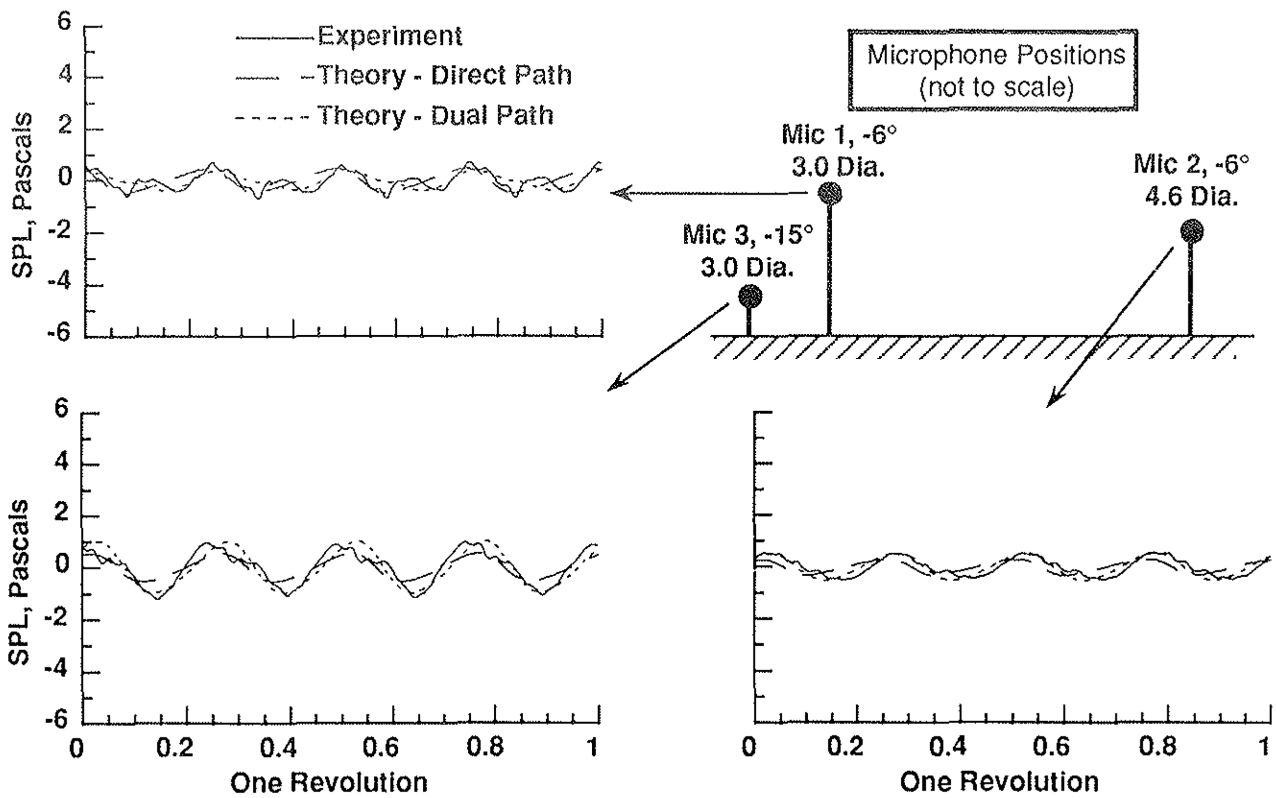

Fig 9. Experiment and theoretical wave shapes, $M_{tip} = 0.544$, $C_T/\sigma = 0.0951$.

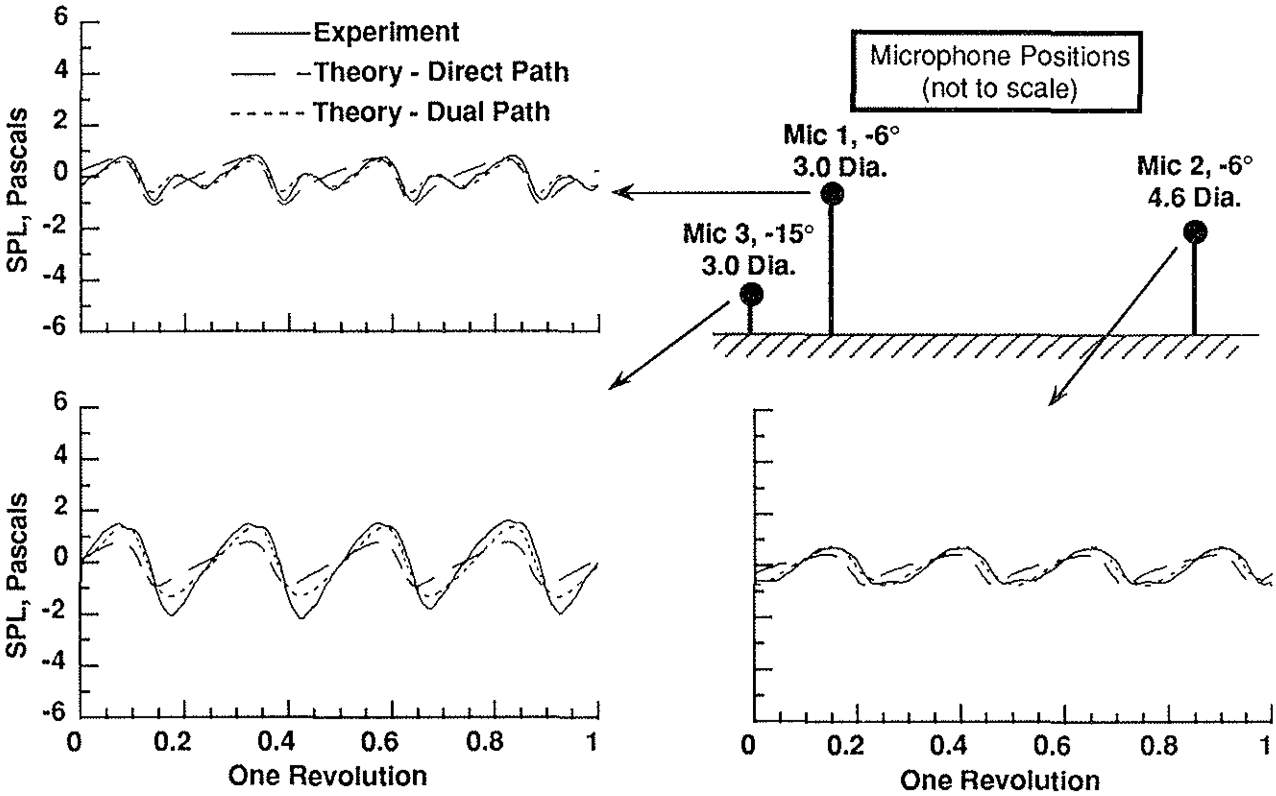

Fig 10. Experiment and theoretical wave shapes, $M_{tip} = 0.630$, $C_T/\sigma = 0.0469$.

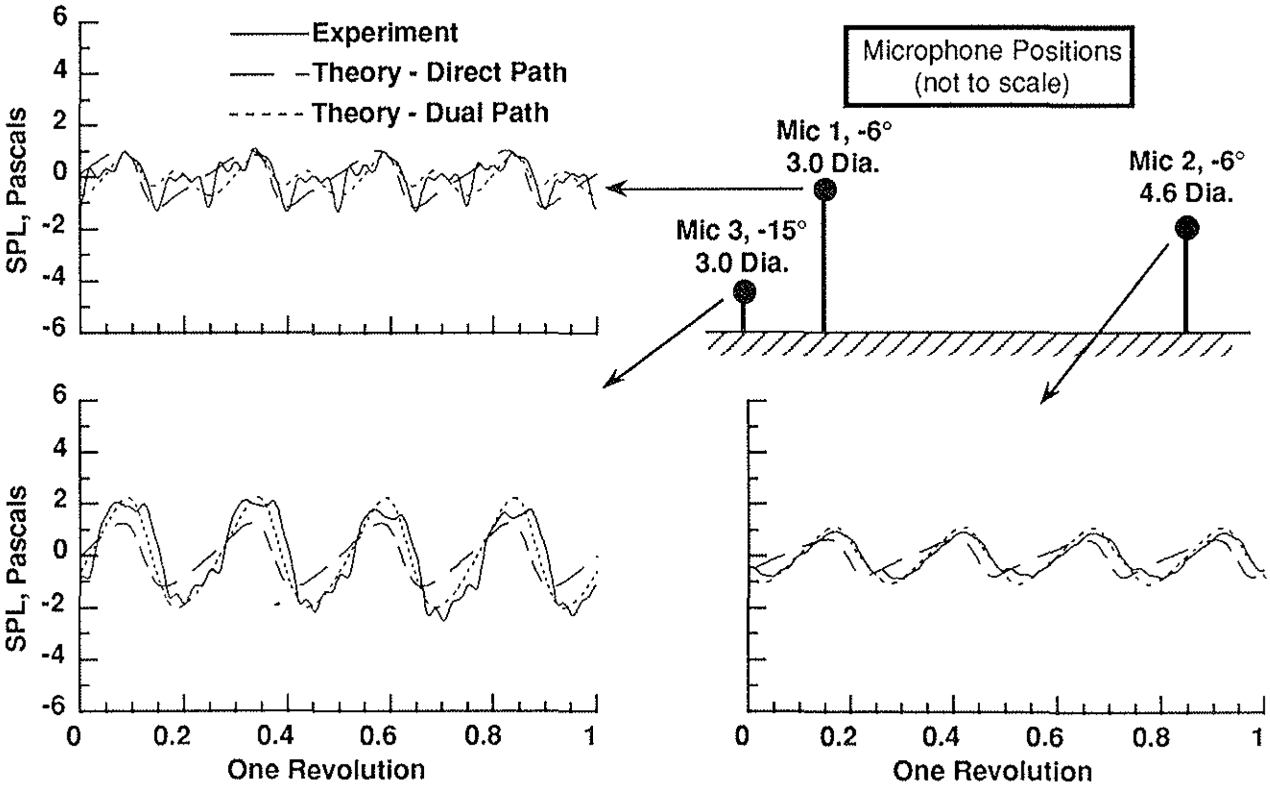

Fig 11. Experiment and theoretical wave shapes, $M_{tip} = 0.630$, $C_T/\sigma = 0.0797$.

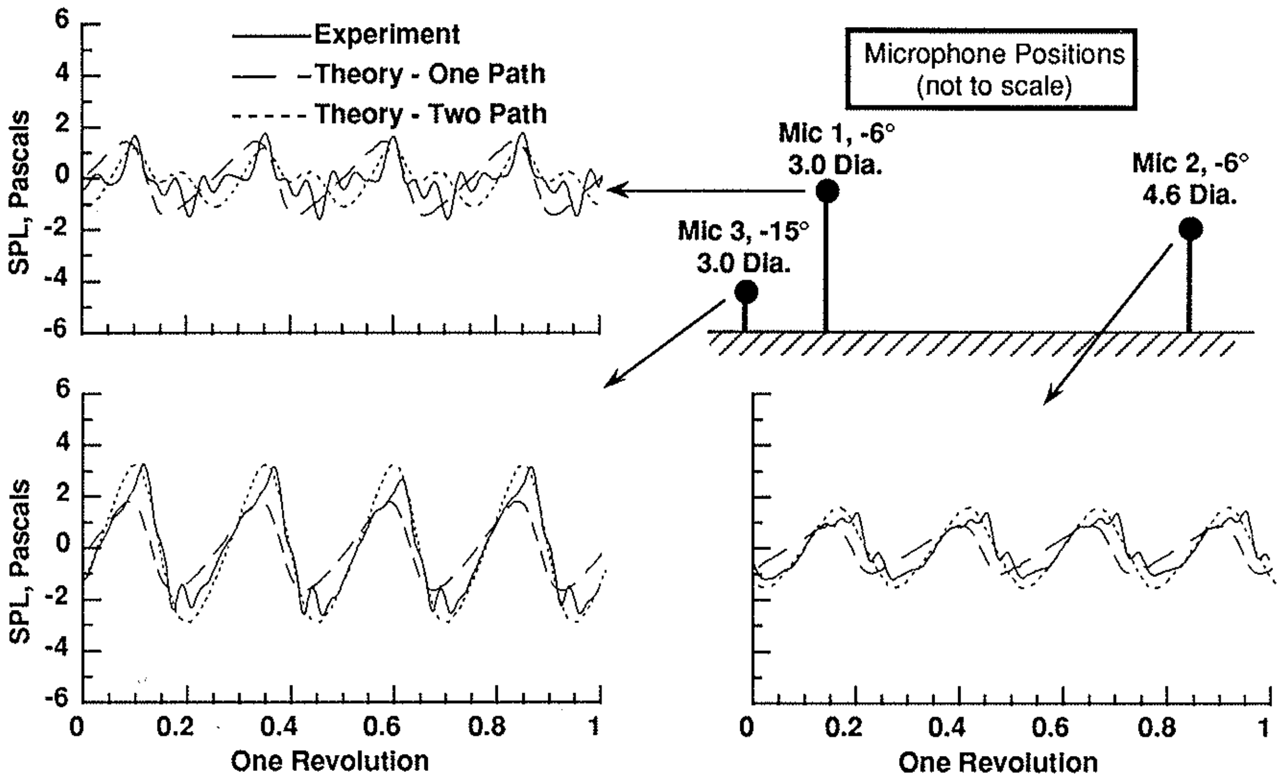

Fig 12. Experiment and theoretical wave shapes, $M_{tip} = 0.630$, $C_T/\sigma = 0.1103$.

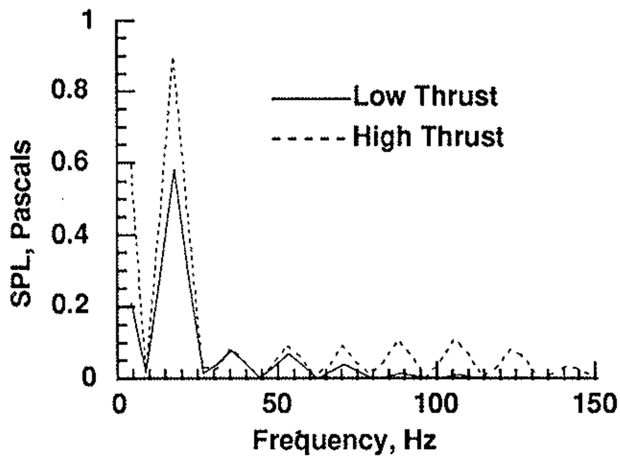

Fig 13. Typical variation of spectra with thrust.

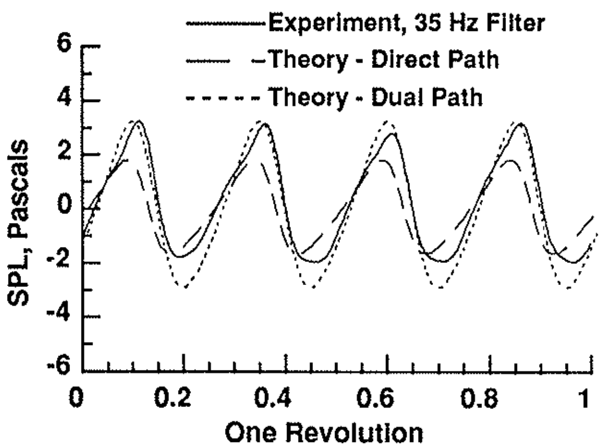

Fig 14. Effect of filtering data at 8/rev (35 Hz).

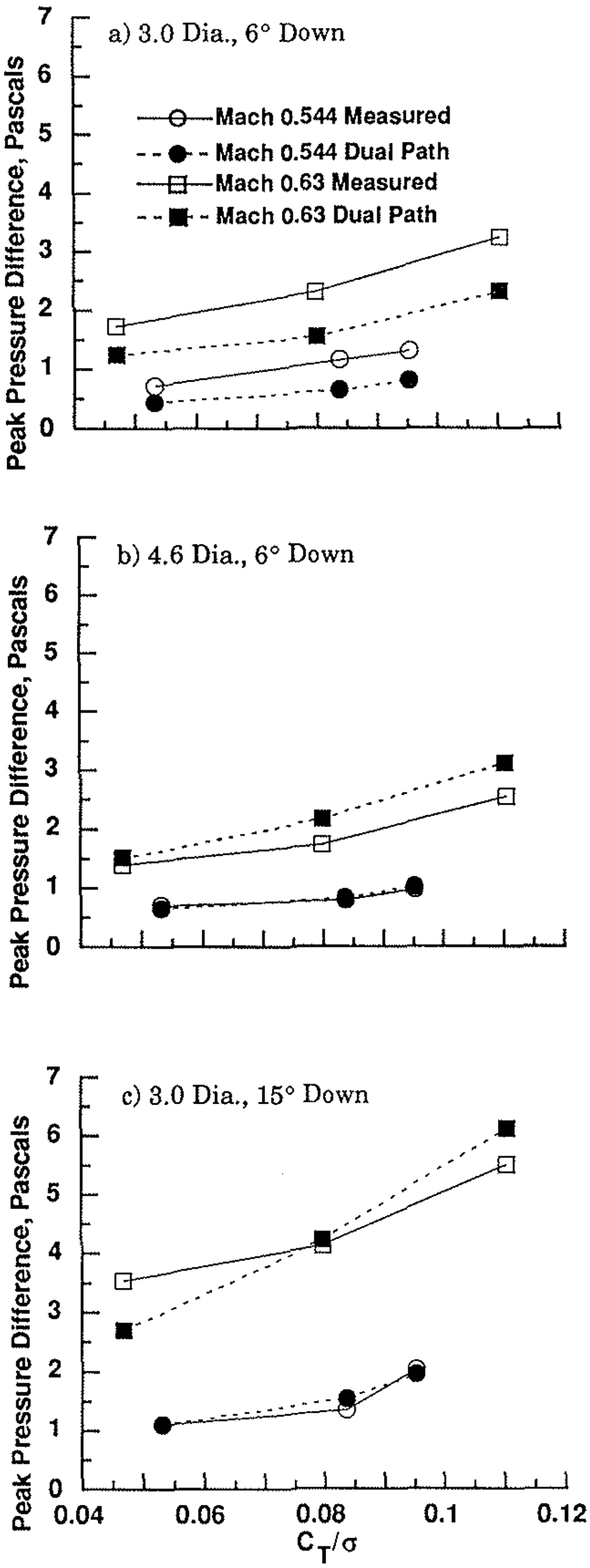

Fig 15. Effect of reflected path on peak pressure differences.

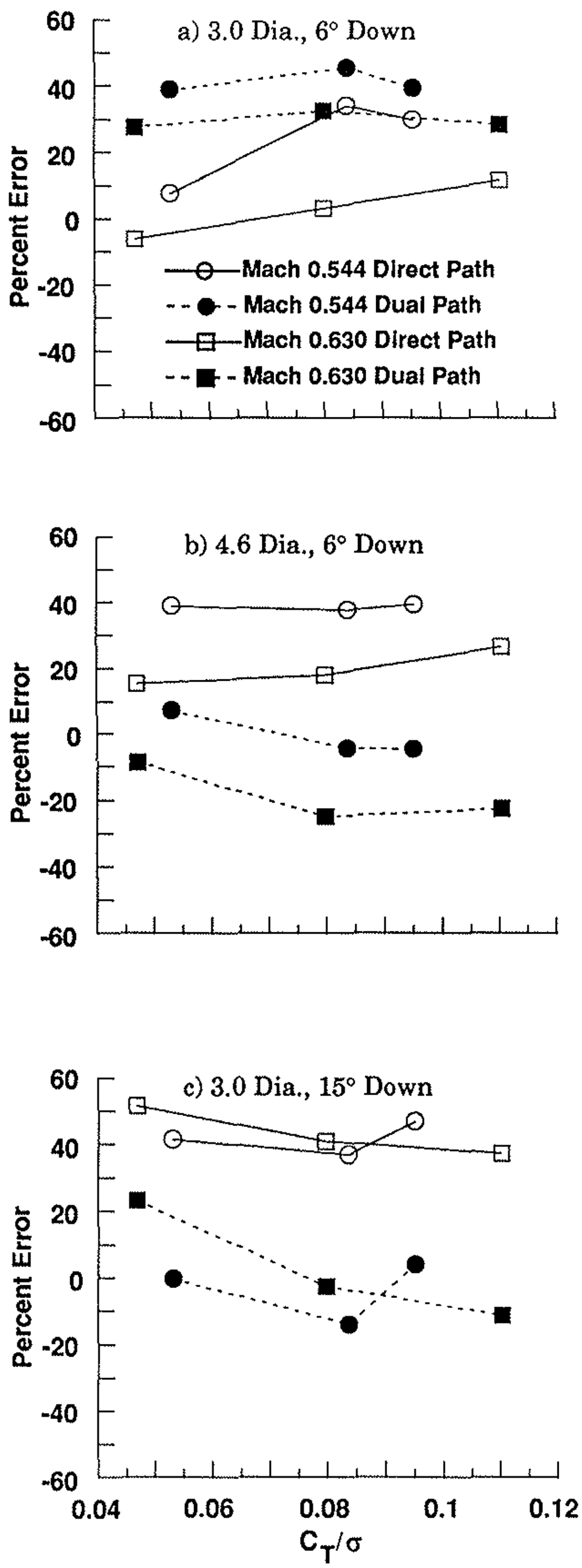

Fig 16. Effect of reflected path on percent error.

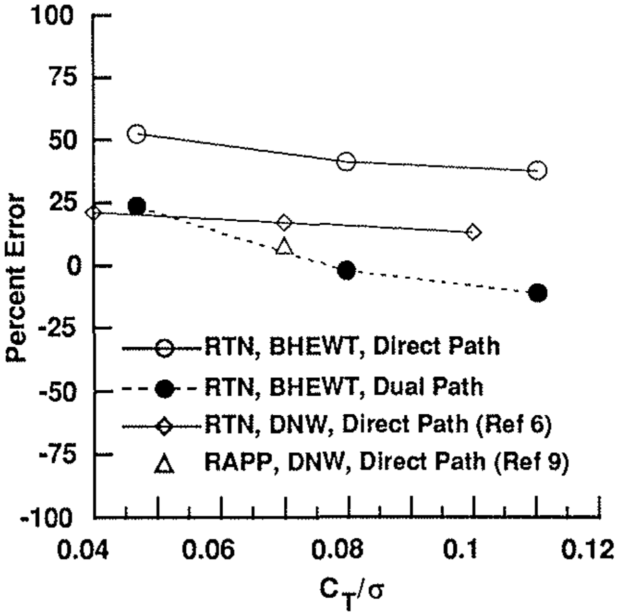

Fig 17. Comparison of percent error with previous investigations for microphone 3 (3.0 Dia., 15° down) at $M_{tip} \approx 0.63$.